Engineering Structures 57 (2013) 609–627

Contents lists available at ScienceDirect

Engineering Structures

journal homepage: www.elsevier.com/locate/engstruct

Pseudodynamic tests on a full-scale 3-storey precast concrete building: Behavior of the mechanical connections and floor diaphragms

Dionysios A. Bournas [a,*], Paolo Negro [b], Francisco J. Molina [b]

[a] Dep. of Civil Engineering, University of Nottingham, NG7 2RD Nottingham, UK
[b] European Laboratory for Structural Assessment, Institute for the Protection and Security of the Citizen, Joint Research Centre, European Commission, T.P. 480, I-21020 Ispra (VA), Italy

ARTICLE INFO

Article history:
Available online 31 August 2013

Keywords:
Precast concrete structures
Pseudodynamic tests
Safecast project
Beam–column joints
Diaphragm
Dry connections
Mechanical connections
Shear walls

ABSTRACT

A full-scale three-storey precast building was tested under seismic conditions at the European Laboratory for Structural Assessment in the framework of the SAFECAST project. The unique research opportunity of testing a complete structural system was exploited to the maximum extent by subjecting the structure to a series of pseudodynamic (PsD) tests and by using four different structural layouts of the same mock-up, while 160 sensors were used to monitor the global and local response of each layout. Dry mechanical connections were adopted to realize the joints between: floor-to-floor, floor-to-beam, wall-to-structure; column (and wall)-to-foundation and beam-to-column. Particular emphasis was given to the seismic behavior of mechanical beam–column connections, as well as to the response of floor diaphragms. Thus, the in-plane rigidity of three pretopped diaphragms with or without openings was assessed. In addition, two types of beam-to-column connections were investigated experimentally, namely hinged beam–column connections by means of dowel bar and emulative beam–column joints by means of dry innovative mechanical connections. Therefore, the seismic behavior of floor diaphragms and pinned beam–column connections in a multi-storey precast building was addressed experimentally. The results demonstrated that the proposed new beam-to-column connection system is a viable solution toward enhancing the response of precast RC frames subjected to seismic loads, in particular when the system is applied to all joints and quality measures are enforced in the execution of the joints.

1. Introduction and background

The research on the seismic behavior of precast concrete structures is very limited if compared to traditional cast-in situ frame reinforced concrete (RC) structures. In fact, in spite of the overgrowing diffusion of this kind of structures, their peculiar characteristics and, in particular, their response to seismic excitation, have not been so thoroughly investigated and univocally determined at present. From a general point of view, there are two alternatives to design precast structures. One choice is the use of precast concrete elements interconnected predominantly by hinged connections, whereas the other alternative is the emulation of monolithic RC construction. The emulation of the behavior of monolithic RC constructions can be obtained using either "wet" or "strong" (dry or partially dry) connections. A "wet" connection between precast members uses cast-in-place concrete or grout to fill the splicing closure. Precast structural systems with wet connections must then comply with all requirements applicable to monolithic RC constructions. A "strong" connection is a connection, not necessarily realized using cast-in situ concrete that remains elastic while designated portions of structural members undergo inelastic deformations under the design ground motion.

The state-of-the-art on the seismic design of precast concrete building structures comprises a limited number of scientific reports. The ATC-8 action – "*Design of prefabricated concrete buildings for earthquake loads*", in the proceedings of its workshop [1] contains eighteen state-of-practice and research papers and six summary papers in particular related to the precast systems in New Zealand, Japan, USA and Europe. Simeonov and Park (1985) [2] addressed the seismic behavior of specific joints used in large panel precast systems of the Balkan region. Another major project, called PRESSS (PREcast Seismic Structural Systems), was made in the 1990s. Specific structural systems with ductile dissipative connections using unbonded PT tendons were addressed by the US and Japanese researchers [3–5]. A relatively recent state-of-art report was published by the fib-Task group 7.3 [6] reporting on (at that time) latest developments on the seismic design of precast concrete building structures in New Zealand, Mexico, Indonesia, Chile, USA, Slovenia, Japan and Italy. In other related documents [5,7,8] special attention is given to the seismic behavior and analytical modeling of the connections. However, although these are the most comprehensive existing documents, they cover only some

* Corresponding author. Tel.: +44 0115 951 4096.
E-mail addresses: dionysios.bournas@nottingham.ac.uk (D.A. Bournas), paolo.negro@jrc.ec.europa.eu (P. Negro), francisco.molina@jrc.ec.europa.eu (F.J. Molina).

0141-0296/$ - see front matter © 2013 Elsevier Ltd. All rights reserved.
http://dx.doi.org/10.1016/j.engstruct.2013.05.046

specific precast structural systems and connections. The Balkan project was strongly oriented to large panel systems, which were extensively used in Eastern Europe but are nowadays outdated. Most other works are limited to moment resisting precast frames based on the emulation of the monolithic structural systems.

The present research is focused on the categories of dry connections, consisting of mechanical devices, which are the most common type in modern precast buildings in Europe. The advantages of dry connections, in terms of quick erection, maintenance, reuse, make them even more appealing in an environmentally friendly, life-cycle performance oriented perspective. Fig. 1 illustrates each category of connection between the different structural elements creating the structural body of a precast building. The *first category* of connections is that between adjacent floor or roof elements. These connections are those affecting the diaphragm action of the roofing of precast structures. The *second category* refers to connections between floor or roof panels and supporting beams. These connections enforce and guarantee the perimetral restraints of the diaphragm made of the panels in its in-plane behavior. The *third category* refers to connections between columns and beams. The beam-to-column joints ensure the required degree of restraint in the frame system. The *fourth category* of connections used to join columns and foundations is typically realized by positioning the precast columns into pocket foundations. Finally, the *fifth category* comprises connections between wall (or cladding panels) and slab elements.

The seismic behavior of the first four categories of connections was investigated in the framework of the SAFECAST project that included, among other tasks, reference pseudodynamic (PsD) tests on a full-scale 3-storey precast concrete building, carried out at the European Laboratory for Structural Assessment (ELSA) of the European Commission in Ispra. This paper investigates the seismic behavior of mechanical beam–column connections, as well as the response of floor diaphragms through the results of those tests.

2. Test structures and investigated parameters

The test structure was a three-storey full-scale precast residential building, with two 7 m bays in each horizontal direction as shown in Fig. 2. The structure was 15 × 16.25 m in plan and had a height of 10.9 m (9.9 m above the foundation level) with floor-to-floor heights equal to 3.5 m, 3.2 m and 3.2 m for the 1st, 2nd and 3rd floor, respectively. The columns cross-section was constant along the height of the structure, equal to 0.50 × 0.50 m, with 1% longitudinal reinforcement (8∅20). Along the main direction there were beams, with a maximum and minimum width of 2.25 m and 1.85 m, respectively. In the orthogonal direction there were slab elements. Detailed description about the geometry and reinforcing details of all structural members used, namely precast concrete columns, beams and walls, is given in the companion paper by Negro et al. 2012 [9]. This paper is focused on the seismic response of: (a) the precast floor diaphragms and (b) the mechanical connections used between precast concrete members.

The SAFECAST specimen was constructed with a special structural layout which allowed four different structural precast systems to be tested. Thus, the behavior of several features was experimentally examined. The possibility of creating rigid floor diaphragms without any concrete topping, a practice that could sensibly speed the construction time of the structure, was investigated through the three different pretopped floor diaphragms that were incorporated among the floors. In addition, the behavior of two types of mechanical beam–column connections was investigated. Firstly, the seismic behavior of "traditional" for the European countries pinned beam–column connections was assessed experimentally for the first time in a multi-storey building. In this case, the columns are expected to work mainly as cantilevers. Then a second type of beam–column connection with innovative mechanical devices which allow for the realization of dry fixed connections was applied and experimentally validated.

The first specimen (prototype 1) comprised a dual frame-wall precast system, where the two precast shear wall units were connected to the mock-up. In this structural configuration, the effectiveness of the three floor systems in transmitting the in-plane seismic storey forces to the vertical elements of the lateral resisting system was investigated. In the second specimen (prototype 2), the building was tested in its most typical configuration, namely with hinged beam–column connections by means of dowel bars. The possibility of achieving emulative moment resisting frames by means of a new connection system with dry connections was investigated in the third and fourth structural layouts. In particular, in the third layout (prototype 3) the beam–column connections were restrained only at the third floor, whereas in the last fourth layout (prototype 4), the connection system was activated in all beam–column joints.

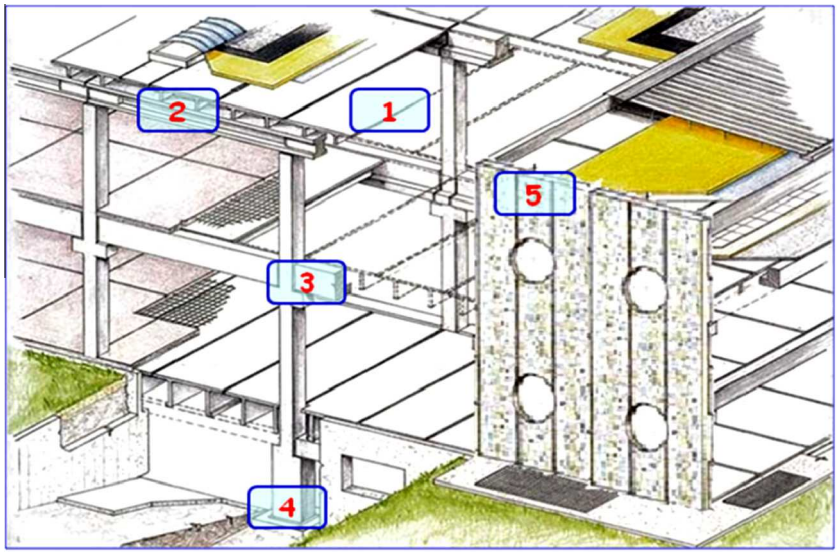

Fig. 1. Categories of connections between the different structural elements of a precast concrete building.

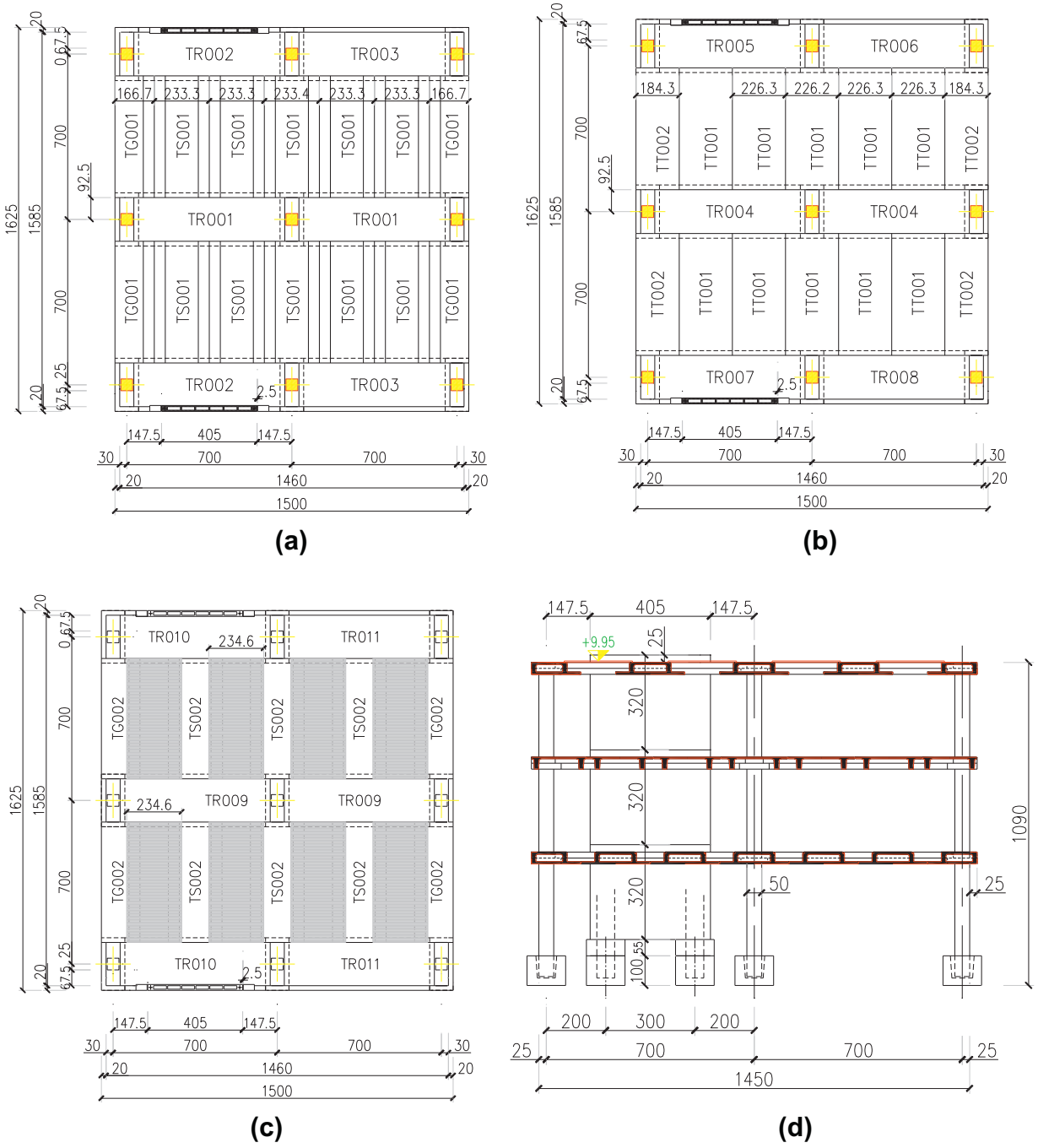

Fig. 2. Plan view of the mock-up at the: (a) First-floor level. (b) Second-floor level. (c) Third-floor level. (d) Section view of the mock-up (dimensions in cm).

2.1. Description of the three floor diaphragms

The floor systems, which were of high interest in this research, were carefully selected to gather the largest possible useful information. To accomplish this, three different pretopped floor diaphragms were incorporated among the floors. The first-floor level incorporated box type elements (TS00X) with a cross-section 0.4 × 2.33 m and a length of 5.13 m (Fig. 2a). The cross section and dimensions of a typical first floor slab element spanning in the transverse (to the loading) direction is illustrated in Fig. 3. A pretopped double-tee diaphragm was located at the second floor of the specimen (Fig. 2b). The 2.33-m-wide units were 5.13 m long with a 50 mm-thick flange and a total section height of 0.4 m (TT00X), as shown in Fig. 4. The pretopped slab elements of the first and second floor were put side by side and welded to each other by 6 L-shape welded elements. Fig. 5 illustrates these slab-to-slab welded connections. Finally, the 3rd floor at 9.9 m was realized with the same box slab elements of the 1st floor (Fig. 3), but not connected among them (Fig. 2c). This last floor system with spaced slab elements was selected to simulate the diaphragms with openings which for architectural reasons are sometimes adopted in the construction practice.

2.2. Description of the mechanical connections

Two different types of beam-to-column connection were used in the test structures. The first type, which corresponds to the most popular connection system in the construction practice in the

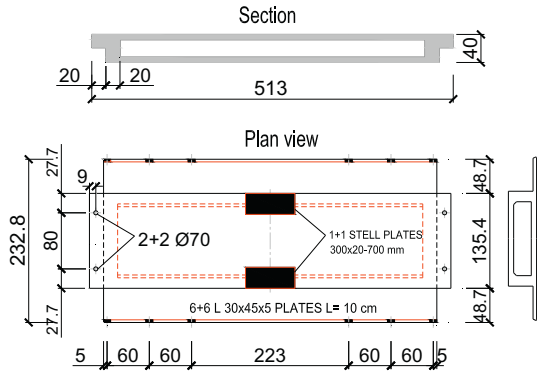

Fig. 3. Cross section and dimensions of the box-type slab elements used in the diaphragms of the first and third floor (dimensions in cm).

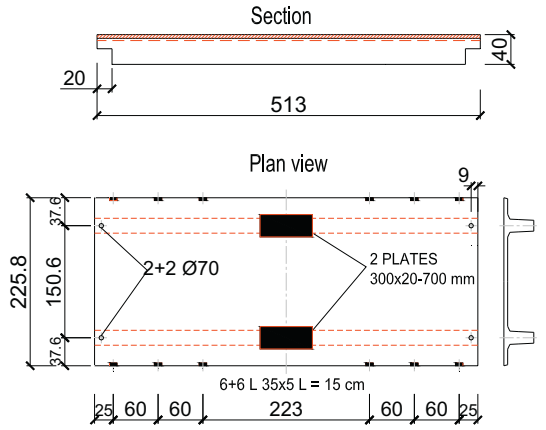

Fig. 4. Cross section and dimensions of the double-tee slab elements used in the diaphragm of the second floor (dimensions in cm).

European countries, comprised hinged beam–column connections by means of dowel bars (shear connectors). This type of connection is able to transfer shear and axial forces both for the gravity and seismic forces and possible uplifting forces due to overturning. By definition, they cannot transfer moment and torsion, although in reality they do transfer a small amount of bending moment. The horizontal connection between the beam and the column was established by means of two vertical steel dowels which were protruding from the column into special beam sleeves. This pinned beam–column connections were constructed by seating the beams on the column capitals and by holding the beam ends in place by the use of the two vertical steel dowels, as shown in Fig. 6a. The dowels were anchored into the capital. The sleeves were filled with a fine non-shrinking grout, while a steel pad 1.0 cm thick was placed between the column and the beam in order to enable relative rotations between the elements. A photo of a typical (central) beam–column joint of the first storey is presented in Fig. 6b. The detail of this pinned beam-to-column connection is presented in Fig. 6c.

The large storey forces which were predicted through non-linear dynamic analyses for the hinged three-storey structure (due to the higher modes effect-[10,11]), resulted also into large actions on the connections. These force demands in the connections remained large when capacity design rules were applied. Thus, it turned out that the required diameters for the dowels were quite large for each storey. In order to have such big diameter at the critical sections, a new dowel was specially developed and used within the SAFECAST project. This dowel has a variable diameter which increases the resisting area in the critical section, namely in the vicinity of the beam–column shear interface, as illustrated in Fig. 6c and d. These dowels work also as shear reinforcement in the case of the structure with fixed joints (prototype 4). Actually, as the joints had not been cast in situ, it would not have been possible to place shear reinforcement to the sections where the beam connects to the column.

The same dowels with increased diameter at the critical section were also used for the connection between slab and beam elements. Each slab element seating on beam capitals was connected through four dowels, namely two on each edge of the slab. Identically, two dowels provided the necessary shear reinforcement area in beam–column connection (Fig. 6b). Table 1 summarizes the

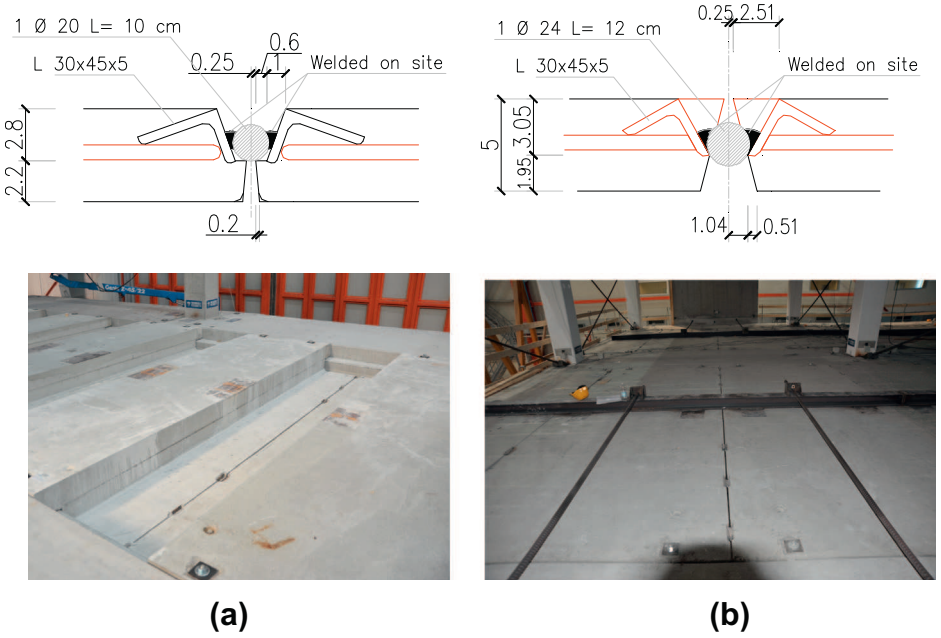

Fig. 5. Slab-to-slab welded connections applied at the: (a) First and third floor. (b) Second floor.

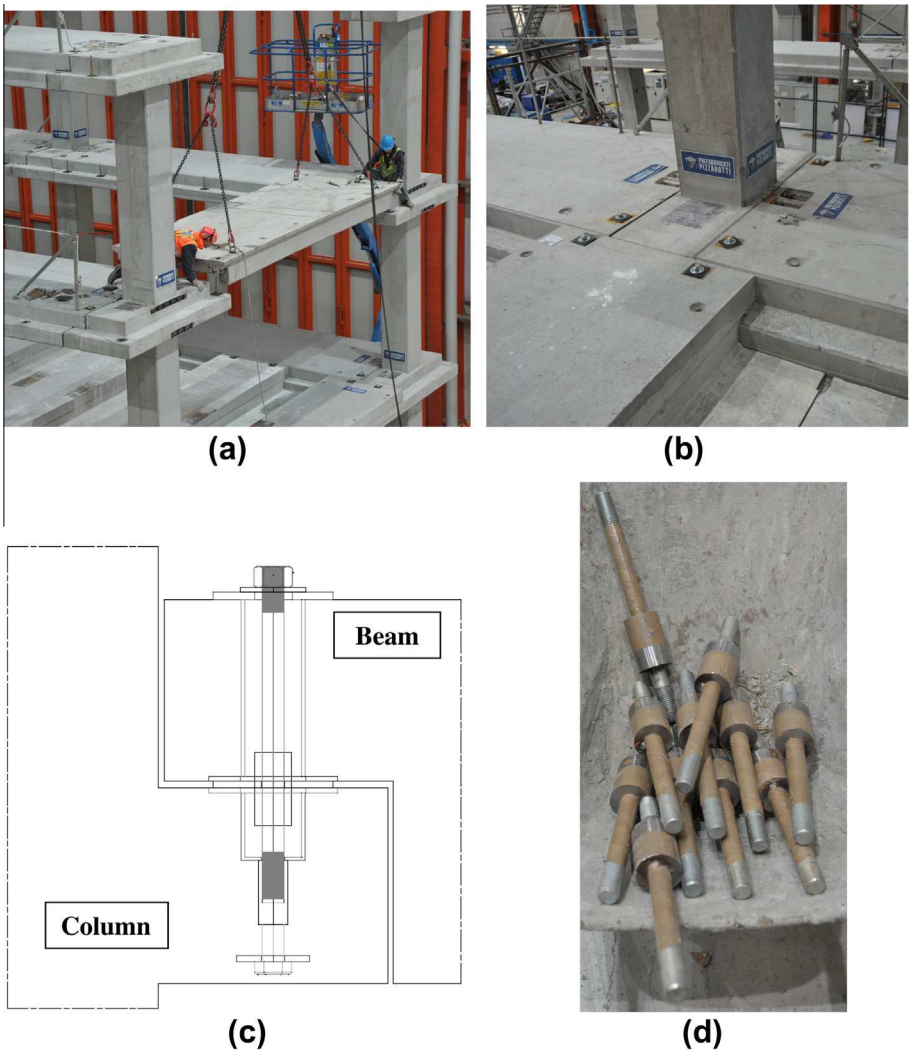

Fig. 6. (a) Seating of a secondary beam on the column capital. (b) A central beam–column joint. (c) Detail of a pinned beam–column joint connection. (d) Special dowels with increased diameter at the critical section.

diameters and the mechanical properties of the steel dowels (Fe430B) used in all pinned beam–column and slab–beam connections.

The second beam–column connection type, which emulates fixed beam–column joints by means of dry mechanical connections, was investigated in the third and fourth structural configurations (prototypes 3 and 4) with the aim of achieving emulative moment resisting frames. Thus, in order to provide continuity to the longitudinal reinforcement crossing the joint, an innovative ductile connection system, embedded in the precast elements, was activated. This connection system comprises four steel rebars slightly enlarged at their ends, two thick steel plates and a bolt that connects the two steel plates, as shown in Fig. 7a and b illustrates the test set-up adopted by Polytechnic of Milan [12] to assess the tensile capacity of the bare connection system without concrete. The results demonstrated a ductile behavior as can be seen in Fig. 7c. When the first rebar started yielding, it initiated elongating and thus transferring force to the other, until both reached yielding. It is important to remark that the rupture mechanism involved exclusively the rebars, with a typical ductile rupture, while the other components of the connection (the two thick plates and the linking bolt) remained intact (Fig. 7d). Table 1 illustrates the results of these (bare) connection systems used in the joints of each floor for creating a moment resisting beam–column connection.

Regarding the realization of this connection system into the mock-up, the bolts that were initially loosen into the joint of

Table 1
Mechanical properties and diameters of steel dowel and emulative connectors.

	Connection type					
	Hinged (beam–column and slab–beam)			Emulative (beam–column)		
Floor	First	Second	Third	First	Second	Third
Dowel diameter (at the critical section) (mm)	24.4 (40)	24.4 (40)	24.4 (52)	–	–	–
Rebar diameter (no. of rebars in the joint) (mm)	–	–	–	Φ25 (4)	Φ16 (8)	Φ20 (4)
Yield stress, f_y (MPa)	265	265	265	417	528	422
Tensile strength, f_u (MPa)	410	410	410	620	634	622
Ultimate strain, ε_u (%)	20.0	20.0	20.0	N/A	10.5	25.2

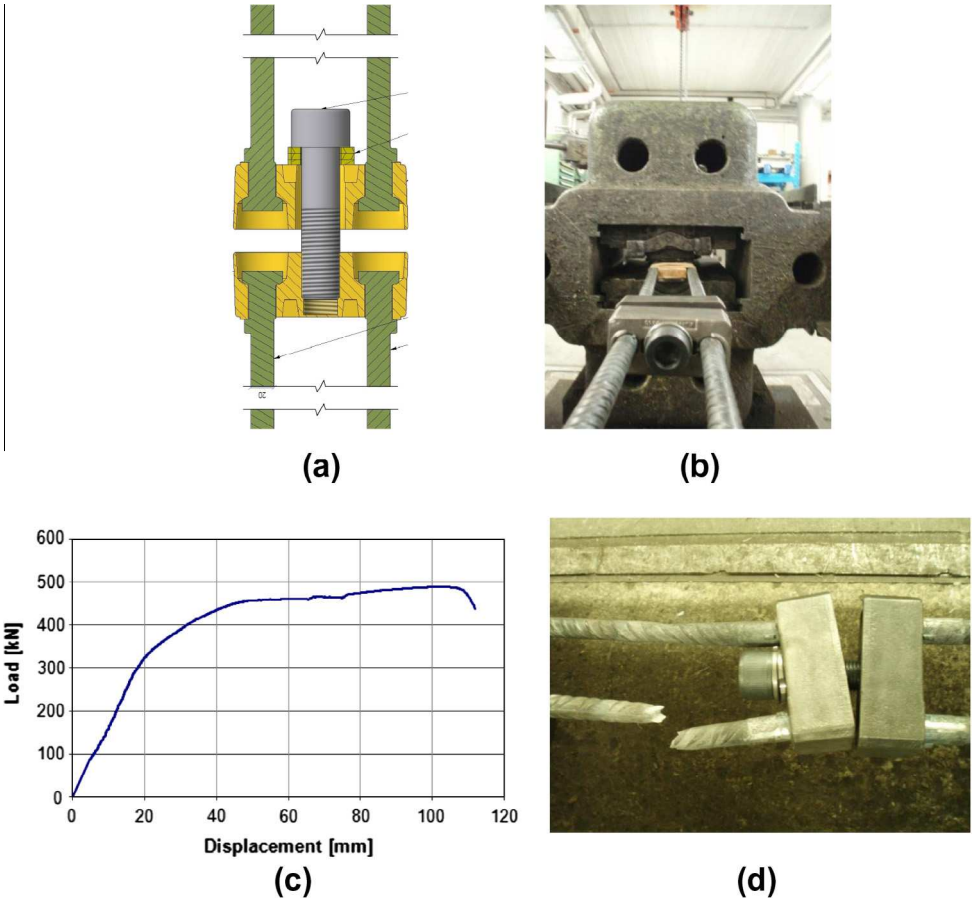

Fig. 7. (a) Connector used to realize dry emulative beam–column joints. (b) Test set-up adopted to assess the tensile capacity of the connection system. (c) Typical load versus displacement curve of the bare connection system. (d) Ductile rupture of the longitudinal rebars. *Source:* [12].

prototypes 1 and 2 were properly screwed (Fig. 8a) and activated (Fig. 8b) to connect the steel devices in the columns and beams. Then, the small (approximately 10–15 mm) gaps between beams and columns were filled by placing a special mortar as shown in Fig. 8c. The average flexural and compressive strength of this mortar were 7.2 MPa and 46.5 MPa, respectively. Fig. 8d presents a scheme of an emulative beam–column joint whereas Fig. 8e illustrates a three-dimensional representation of the mechanical connector in a beam–column joint.

3. Experimental program

The prototypes were subjected to a series of PsD tests. The seismic action was simulated by a real accelerogram modified to be compatible with the EC8 response spectrum for soil type B [9]. Two PsD tests at peak ground accelerations (PGAs) of 0.15 g (Prot1_0.15g) and 0.30 g (Prot1_0.30g) were initially conducted on prototype 1. The same test sequence was repeated (when the walls were disconnected) for prototype 2 (Prot2_0.15g and Prot2_0.30g). Prototype 3 was subjected only to the higher intensity earthquake of 0.30 g (Prot3_0.30g), whereas prototype 4 was tested at the PGAs of 0.30 g (Prot4_0.30g) and 0.45 g (Prot4_0.45g). Finally, a sequence of cyclic tests was performed, controlling the top displacement of the structure and constraining the floor forces to an inverted triangular distribution, in order to approach the ultimate capacity of the structure.

The lateral displacements were applied on the mid axis of the two bays by two hydraulic actuators. Steel beams were placed along the two actuator axes to connect all the floor elements and distribute the applied forces. An instrumentation network of 175 channels was used to measure: (1) The horizontal displacements of the three frames of the structure (two externals and one central) at the level of each storey. (2) Absolute rotations within the plane of testing of all ground storey columns, 300 mm above their bottom. (3) Absolute rotations within the plane of testing for the beams and columns in the vicinity of all beam–column joints of the central frame and one of the external frames. (4) The beam-to-column joint shear displacement measured in selected beam-to-column joints. An overview of the instrumentation set up adopted is presented in Appendix A.

The PsD testing method used, the test set-up adopted as well as the selected input motion are described in detail in the companion paper [9].

4. Experimental results and discussion

Detailed results about the global PsD response of the four prototypes are given in the companion paper. In this paper the authors focus on the seismic behavior of the mechanical connections used between the precast elements, as well as on the seismic response of the floor diaphragms.

4.1. Global behavior of the prototypes

The global response of all prototypes tested under the PGA of 0.30 g is summarized in Fig. 9 in the form of base shear force versus roof displacement hysteresis loops. Key results about prototypes' general behavior in every test are also summarized in Table 2. They

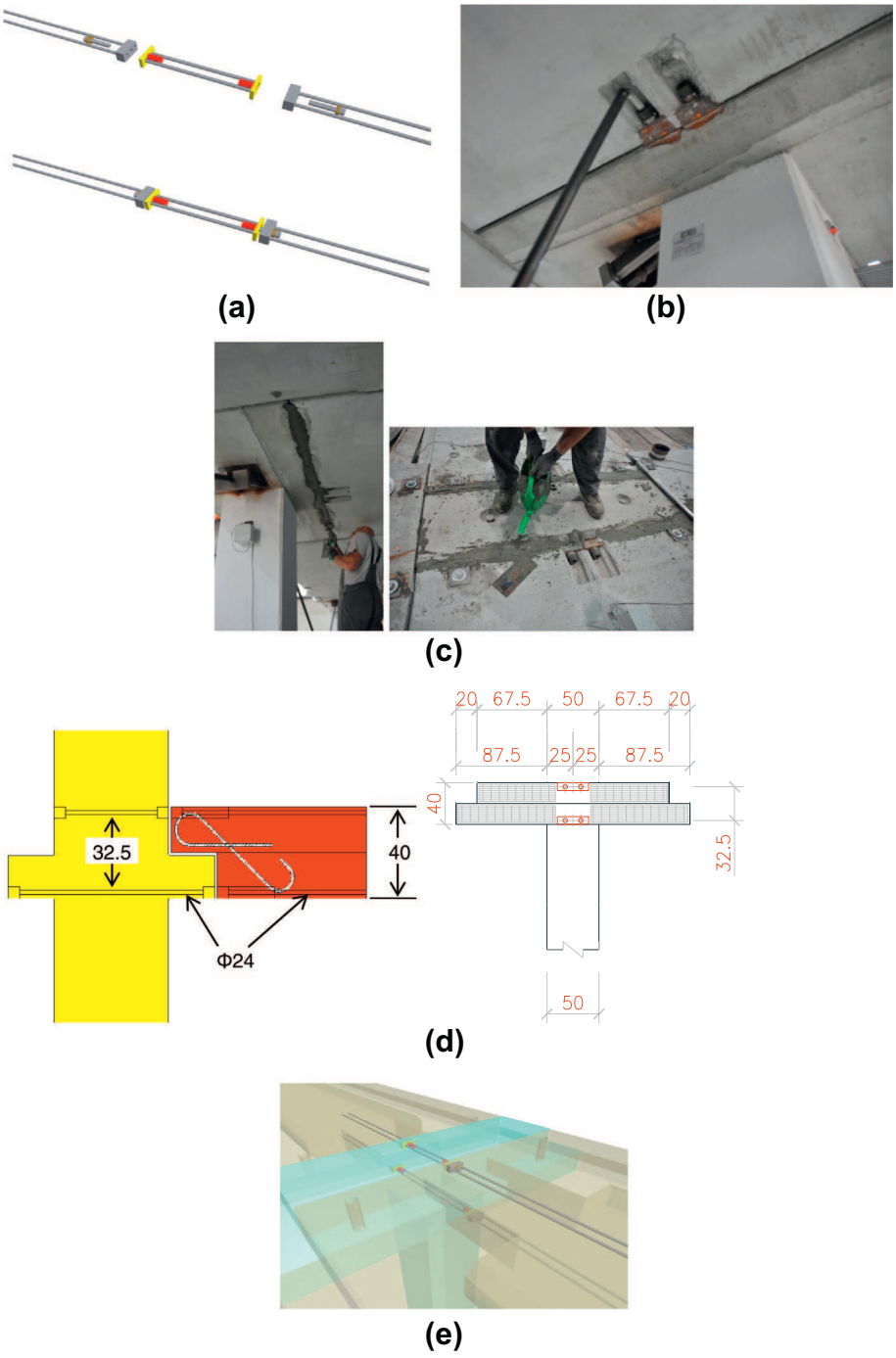

Fig. 8. (a) Loosen and activated connection system in its bare configuration. (b) Activation of the loosen bolts to provide continuity to the longitudinal bars crossing the beam–column joint. (c) Filling the gaps in the joints with mortar. (d) Detail of an emulative beam–column joint. (e) Three-dimensional representation of the mechanical connector in a central beam–column joint.

include: (a) The maximum base shear in the two directions of loading. (b) The peak roof displacement. (c) The maximum storey forces recorded in each floor. (d) The maximum rotation measured with inclinometers 300 mm above the base of the ground floor columns. (e) The curvature ductility factor, which is defined as $\mu_\phi = \phi_{max}/\phi_y$, where ϕ_y and ϕ_{max} are the mean curvatures of the column at yield (calculated with cross-section analysis), and the maximum curvature measured during the tests, respectively. The experimental curvature was derived from the relative rotation measured over the lower 300 mm of the column above the base, which includes the rotation of the column section at the face of the footing and the effect of bar pull-out from the base.

4.2. Response of the floor diaphragms

Fig. 10 presents the displacement histories of the three frames (two externals and one central) at the floor levels for prototype 1 subjected to the 0.30 g seismic excitation. As it can be observed, in the first and second floor the displacement of each frame was practically the same, a fact which indicates that the in-plane rigid-

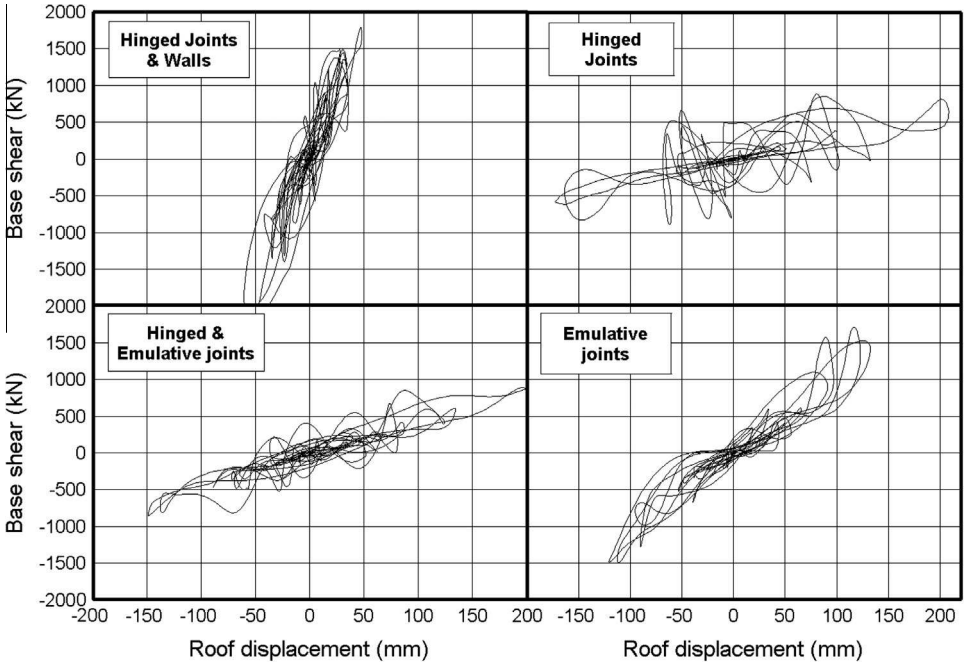

Fig. 9. Base shear versus roof displacement response of the four structural systems at PGA of 0.30 g.

ity of the diaphragms was not impaired by their connection with stiff RC walls. In the third floor, however, the maximum displacement of the middle frame was 20% higher than the corresponding displacements of the two external frames. The openings in the diaphragm of the third floor reduced its in-plane stiffness and consequently the two external frames connected to the shear walls deformed less than the central frame.

The displacement calculated as the third DoF in the PsD 3-DoF equation of motion and applied to the third floor at the axes of the actuators, was approximately equal to the average of the displacement measured in the external and central frames (which is also an approximation of the average displacement of the floor mass). In fact, the third DoF displacement was 9.1% lower than the corresponding displacement of the central frame and 9.3% higher than the average displacement of the two external frames. It is important to note here that according to EC8, a diaphragm is taken as being rigid, if, when it is modeled with its actual in-plane flexibility, its horizontal displacements nowhere exceed those resulting from the rigid diaphragm assumption by more than 10%. Consequently, this condition of EC8, for assuming rigid in their planes floor diaphragms, was met herein even for the case of the diaphragm with openings, connected to stiff precast RC walls and subjected to the 0.30 g earthquake. This seismic intensity corresponds to the ultimate limit state.

Table 3 summarizes the maximum frame and absolute displacements of the third floor measured experimentally in all prototypes and tests performed. Clearly, once the shear walls were disconnected from the mock-up, the diaphragm action was substantially improved in the remaining prototypes 2, 3 and 4. In the latter case, the horizontal displacement in the three frames was practically the same since the seismic storey forces were transmitted from the diaphragm to the beams and finally to the columns (more) uniformly.

4.3. Response of the beam–column joints

4.3.1. Hysteretic behavior of the joint

Within the assumption of concentrated floor mass at the actuators axes in the PsD testing set-up, the in-plane behavior of the floors was rigid as it was confirmed experimentally here for all floors of the prototypes 2, 3 and 4 (Table 3) and the seismically induced deformation was uniformly distributed. Based on the large in-plane stiffness of the floor (rigid diaphragm) and the elastic response of the connections (as explained below), the storey forces are thus equally distributed among all columns. This means that the capacity demand on the connection is equal to the total storey force divided by the number of columns and the number of connections which are attached to a column. Therefore, in the following plots, the force at the joint was approximately taken equal to the storey force divided by nine (i.e. the number of columns). In addition, by combining the measurements of the LVDTs and inclinometers fixed at selected beam–column joints of the second and third floor (see Appendix A); it was possible to calculate the joint horizontal and vertical slip. The joint horizontal slip was calculated by subtracting from the horizontal LVDT recording its component which was attributed to the relative beam–column rotation. The last was calculated on the basis of the inclinometers fixed on the beam–column joint.

In Fig. 11, the diagrams of the joint shear force versus the joint slip (horizontal displacement) loops are presented for an external beam–column joint (joint 13-see in the Appendix A) of the third floor, subjected to the 0.30 g (prototypes 2, 3 and 4) and 0.45 g seismic excitations (prototype 4), respectively. The horizontal opening of the joint (joint slip) was as expected higher in the case of prototype 2 (Fig. 11a) with pinned connections. At the 0.30 g test, the average joint slip among the beam–column joints of the third floor that were monitored, was 7.1 mm, 4.7 mm and 1.99 mm, for prototypes 2, 3 and 4, respectively. Consequently, for the same seismic input motion of 0.30 g, the joint slip was reduced dramatically in prototype 4 with moment resisting joints, that is 3.5 times lower than its counterpart with hinged beam-to-columns joints. A similar trend was observed for the joint axial elongation which from 1.91 mm in prototype 2, was reduced to 0.97 mm in prototype 3 and 0.78 mm in prototype 4, when the mechanical connection system (Fig. 8) was activated in all joints. The joint axial elongation that is (essentially) attributed to the relative beam–column rotation (calculated by multiplying the relative beam–column rotation with half the beam depth) can be approximately considered equal the elongation of a dowel well an-

Table 2
Summary of test results.

Specimen notation	Maximum base shear (kN)		Peak roof displacement (mm)		Maximum storey forces (kN)						Maximum rotation at the column base, θ_{max} (%)	Curvature ductility factor $\mu_\phi = \phi_{max}/\phi_y$
	Pull	Push	Pull	Push	Pull			Push				
					1st	2nd	3rd	1st	2nd	3rd		
Prot1_0.15g	1340	−1457	21.9	−16.8	491	595	688	−475	−577	−581	0.08	0.29
Prot1_0.30g	1780	−2146	48.2	−60.3	722	788	1027	−848	−974	−1166	0.18	0.73
Prot2_0.15g	500	−442	97.4	−86.6	345	336	325	−303	−284	−261	0.28	1.44
Prot2_0.30g	882	−895	208.2	−172.9	795	649	577	−769	−676	−599	0.66	2.86
Prot3_0.30g	889	−859	198.7	−148.4	651	561	540	−691	−453	−471	0.85	3.71
Prot4_0.30g	1715	−1454	132.5	−121.2	921	828	777	−629	−686	−600	0.95	3.85
Prot4_0.45g	1846	−1902	189.3	−206.5	924	794	1133	−848	−855	−772	1.89	7.33
Cyclic test	2237	−2031	388.1	−415.6	754	1494	974*	−677	−1357	−934*	6.11	22.3

* Maximum force recorded during displacement amplitude of ±300 mm.

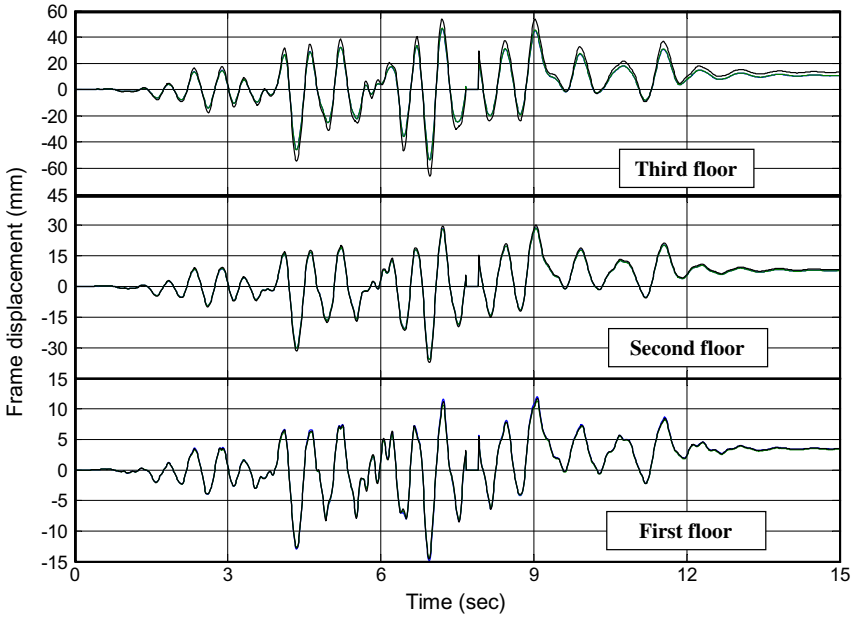

Fig. 10. Frame displacement histories of prototype 1 at PGA 0.30 g.

Table 3
Frame and absolute displacements in the third floor.

Specimen notation	Third floor horizontal displacement (diaphragm with openings) (mm)				Maximun difference in the ratio of displacements (%)		
	South frame	Central frame	North frame	DoF	Central to external frame	DoF to central frame	DoF to external frame
Prot1_0.15g	19.4	21.9	18.2	19.4	20.3	−8.80	6.60
Prot1_0.30g	50.2	59.8	49.7	54.3	20.3	−9.10	9.25
Prot2_0.15g	104.3	105.4	104.5	106.7	1.01	1.23	2.30
Prot2_0.30g	188.1	189.8	189.9	190.5	1.00	0.35	1.28
Prot3_0.30g	173.9	175.9	173.8	173.6	1.21	−1.31	−0.11
Prot4_0.30g	125.9	129.1	126.0	126.9	2.54	−1.70	0.80
Prot4_0.45g	195.6	201.0	195.9	197.9	2.80	−1.54	1.12
Cyclic test	403.5	404.0	402.5	401.2	0.37	−0.69	−0.57

chored to its ends. Thus, by dividing by its anchorage length (l_d = 270 mm – Fig. 6), the average dowel axial strains can be estimated. For prototypes 2, 3 and 4 the relative values were equal to 0.71%, 0.36% and 0.28%, respectively.

Fig. 12 illustrates the joint shear force versus joint slip and axial displacement recorded at the second floor of an external and a central joint (joint 7 and joint 8 – see Appendix A), during the cyclic test. It should be pointed out that the strength of the connections (as it is calculated below) was higher than the capacity of the columns even at very large relative beam-to-column rotations. Plastic hinging was formed at the base of the columns well before the maximum capacity of the connections was reached.

The cyclic strength $D_{u,cyc}$ of the connection for well detailed joints (large concrete cover and sufficient confinement), can be

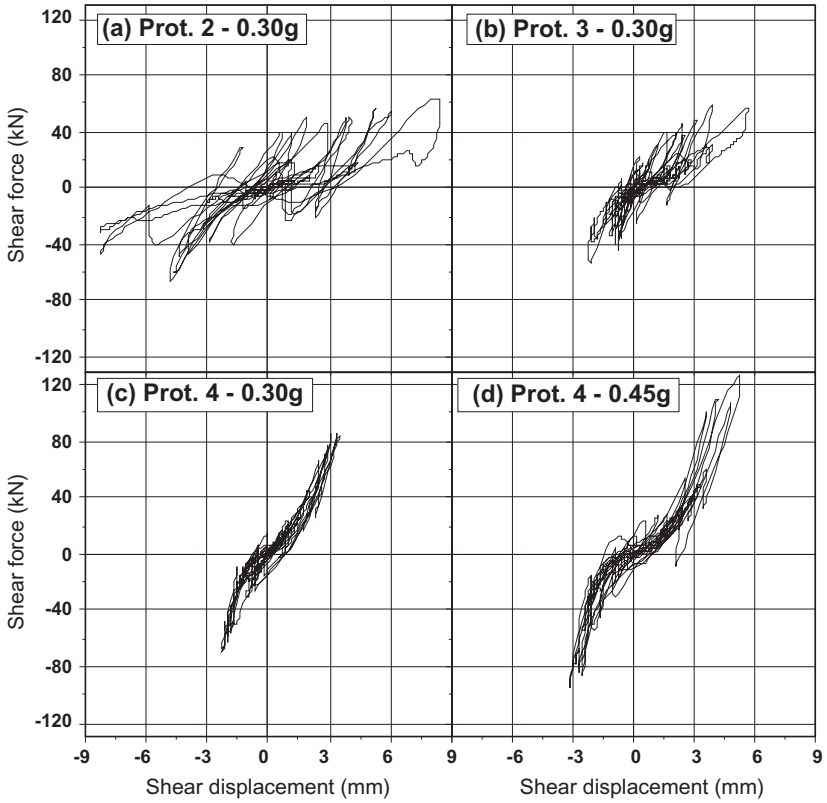

Fig. 11. Joint shear force versus the joint slip loops for an external beam–column joint (J13) of the third floor of: (a) Prototype 2 at PGA 0.30 g. (b) Prototype 3 at PGA 0.30 g. (c) Prototype 4 at PGA 0.30 g. (d) Prototype 4 at PGA 0.45 g.

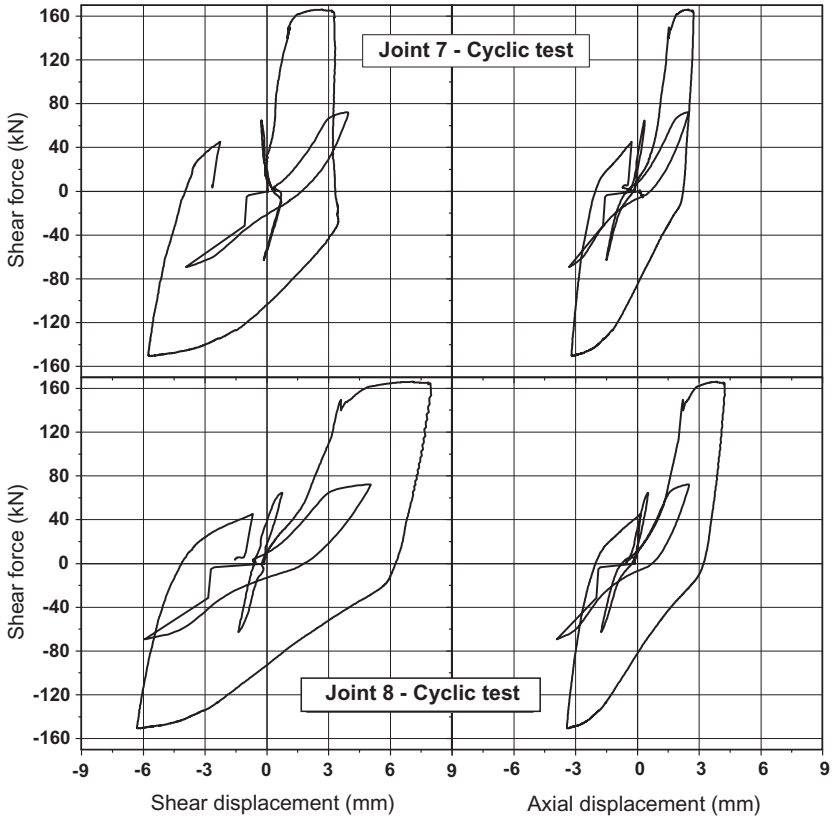

Fig. 12. Joint shear force versus joint slip and axial displacement recorded at the second floor of an external and a central joint during the cyclic test.

Table 4
Maximum recorded rotations at joints of the first floor.

Joint rotations at the first floor	Joint 1 (rad × 10^{-3})		Joint 2 (rad × 10^{-3})		Joint 3 (rad × 10^{-3})		Joint 4 (rad × 10^{-3})		Joint 5 (rad × 10^{-3})		Joint 6 (rad × 10^{-3})		Average (rad × 10^{-3})		Column to beam rotation ratio
	Beam	Col.	Beam	Col.	Beam	Col.	Beam	Col.	Beam	Col.	Beam	Col.	Beam	Col.	
Prot.1_0.30g	0.5	5.3	0.7	5.1	0.8	5.2	0.5	5.3	0.7	4.8	0.6	5.1	0.63	5.1	8.1
Prot.2_0.30g	2.1	19.1	2.2	18.3	2.2	18.2	1.7	18.3	2.2	17.2	2.2	18.6	2.1	18.3	8.7
Prot.3_0.30g	4.9	32.9	5.0	31.5	5.1	31.8	4.2	32.5	2.7	19.4	2.6	21.1	4.1	28.2	6.9
Prot.4_0.30g	9.0	23.5	2.9	21.4	6.2	22.3	9.0	22.7	9.6	13.8	0.86	17.3	4.1	20.1	4.9
Prot.4_0.45g	10.0	36.4	3.2	33.4	7.9	33.9	9.7	35.2	2.2	21.3	N/A	25.7	6.7	31.0	4.6
Prot._Cyclic	19.7	86.0	7.0	83.4	24.7	84.5	15.4	83.4	4.0	53.5	15.3	50.6	14.5	73.5	5.1

estimated according to the following expression proposed by Vintzeleou and Tassios [14] when the calculation of the dowel's shear strength is of concern:

$$D_{u,cyc} = 0.50 \cdot 1.30 d_b^2 \sqrt{f_{ck} f_{sy}} \quad (1)$$

where f_{ck} and f_{sy} are the characteristic strengths for concrete and steel (units in MPa), and d_b is a diameter of the dowel (units in mm). According to the results of Eq. (1), the cyclic shear strength of an external beam–column connection (2 dowels) of the first and second floor is equal to 271 kN. Note that in the third floor larger diameter dowels were used, while in the central beam–column joints where the connection is realized with 4 dowels. As a result, the strength of the beam–column connection is in both cases superior. Therefore, it appears that the response of the beam–column connections in terms of shear capacity remained in the elastic range in all prototypes, however, significant cracking appeared in the vicinity of the first floor's emulative joints as explained in next sections.

4.3.2. Column versus beam rotation

In a perfectly hinged beam-to-column joint there is no moment transfer to the beam and consequently the latter does not rotate. On the contrary, in a monolithic-moment resisting-connection the beam is fixed to the column and ideally rotates as much as the latter does. The rotations measured experimentally in many joints of the three floors, though, did neither confirm the first nor the second hypothesis concerning fully hinged or fixed joints. Table 4 lists the maximum values of columns and beams rotation recorded in the vicinity of six (out of nine) beam–column joints of the first floor during the PsD and cyclic tests. Table 4 gives also the average beam and column rotation, as well as the column-to-beam rotation ratio. In prototypes 1 and 2 with hinged joints, the beam rotation is very small (yet not negligible) and the ratio of the column-to-beam rotation is about 8.5. Once the mechanical connection devices were activated in all beam–column joints (prototype 4), notably higher activation of the first floor beams in the frame behavior was achieved. In particular, for the same seismic excitation of 0.30 g, the beams rotation in the first floor of prototype 4 was doubled in comparison with those measured in prototype 2, while the ratio of column to beam rotation was reduced to approximately 5.

Fig. 13 presents the evolution of the column and beam rotation in a typical (external) joint of the first floor, for all structural configurations subjected to the 0.30 g seismic excitation. Once more two main aspects can be observed: (1) higher participation of the

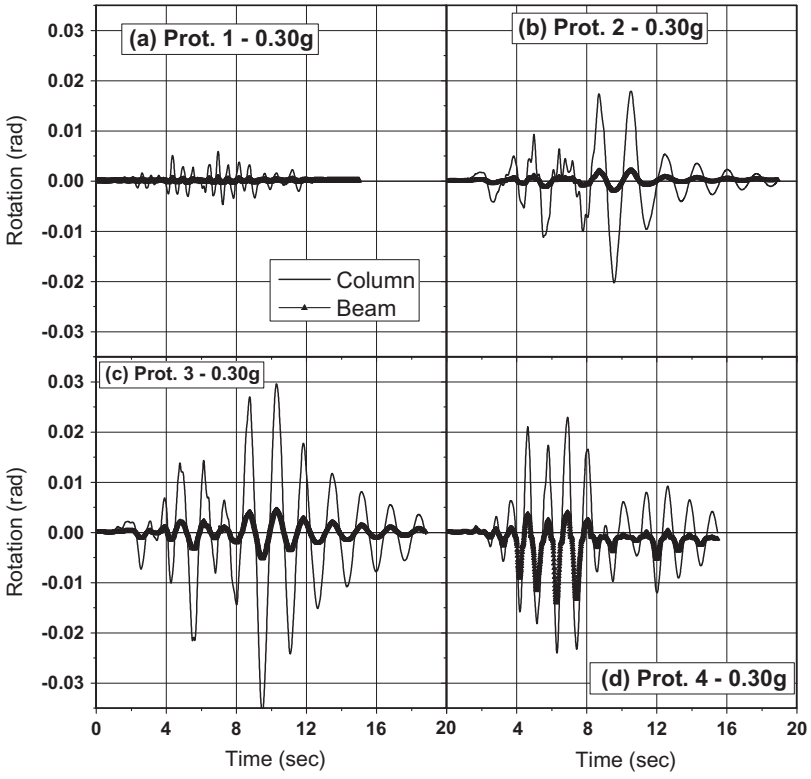

Fig. 13. Evolution of column and beam rotation in first floor's joint at PGA of 0.30 g for: (a) Prototype 1. (b) Prototype 2. (c) Prototype 3. (d) Prototype 4.

Fig. 14. Well executed and non satisfactory-filled joints as revealed at the demolition of the mock-up.

beams in the frame behavior of prototype 4; and (2) the beam–column emulative joint response in prototype 4 quite different from a rigid joint. It should be pointed out that the execution of this mechanical connection has no quality control or certification for the time being. The state of the mortar filling in the gaps between columns and beams was not identical in all joints and in some cases the penetration of mortar in the gaps was poor. For example Fig. 14 illustrates both cases of a well-executed joint (Fig. 14a), where the mortar successfully penetrated in the gaps between columns and beams, and a non-satisfactorily-filled joint (Fig. 14b), as revealed during the demolition phase of the mock-up. This resulted into a semi-rigid beam–column joint with asymmetric (in the two directions of loading) and unequal (between beams and columns) rotations, as shown in Fig. 13.

The above findings were exploited in calibrating numerical models for both types of beam-to-columns connections by the University of Ljubljana (UL) research group [15]. For the case of hinged connections, a distributed plasticity numerical model, which incorporates a force-based beam–column element (OpenSees) with five integration points, was modified accordingly to consider the increased stiffness of the structure that was caused by the partial connection of the beam–column connections. This was practically realized by adding zero-length elements (rotational springs) at the locations of the beam–column hinges, with a linear elastic relationship for the rotational degree of freedom to model the partial connection, as shown in Fig. 15a. The elastic stiffness of the spring was calibrated from the UL research group with the experimental results of prototype 2 and the elastic stiffness (k_M), for such hinged-beam column joints, which yielded the best fit to the experimental results, was equal to 1600 kN m/rad. For the second connection type which emulates fixed joints, the experimental results of prototypes 3 and 4 demonstrated that there was an initial gap in the moment–rotation response as well as a pinching effect. The gap was explained as an initial opening at the location of the beam–column joint, resulting into an unrestrained rotation between the beam and the column, while the pinching effect was attributed to the subsequent damage (falling) of the mortar filling between the beams and the columns. The gap and the pinching effect were introduced in the numerical model [15] by adopting the joint moment–rotation relationship of Fig. 15b. The length of the gap and the size of the initial stiffness were calibrated from UL with the experimental results of prototype 4, and were found for such mechanical semi-rigid connections, equal to $\theta = 0.005$ rad and $k_{initial} = 4000$ kN m/rad, respectively. Naturally, more details about both numerical models can be found in [15].

4.3.3. Energy dissipation

To further evaluate the effectiveness and the seismic response of both types of beam–column connections, the cumulative dissipated energies – computed by summing up the area enclosed within the shear loads versus inter-storey drifts curves – were recorded for each prototype subjected to the 0.30 g PGA seismic excitation and plotted in Fig. 16. Fig. 16 decomposes also the total energy into the energy dissipated by the three individual floors. With the exception of prototype 1, all other layouts displayed considerably higher energy dissipation in the first floor compared to the second and third one. This is attributed to the flexural cracking and yielding which was mainly concentrated at the base of the ground floor columns for the prototypes 2, 3 and 4, as it is explained in the companion paper [9]. The energy dissipation in the third floor was identical for all specimens. In prototype 4, the energy dissipated in the second and first floor was respectively 53% and 72% higher than the energy dissipated by prototype 2 in the corresponding floors. Beyond the flexural cracking and yielding at the base of the ground floor columns, the enhanced energy dissipation in the first floor of prototype 4, is also ascribed to the higher activation of the beams (Fig. 13) and their considerable flexural cracking achieved at the first floor (column to beam rotation ratio 5).

4.3.4. Damage in the connections

Despite the fact that the strength of the beam–column connection was not approached during the final "funeral" cyclic test, the emulative joints experienced inelastic behavior and cracking. Especially at the first floor level, where higher bending moments were developed, the cracking in the vicinity of the mechanical devices was extensive. The flexural cracking at the joints started at the initial stages of loading, with the main flexural crack which was always appearing at the column capital–beam interface, where mortar was poured to fill the gaps. In addition, large inclined cracks, propagating in the concrete surface as a result of high pull-out forces of the longitudinal reinforcement crossing the joint,

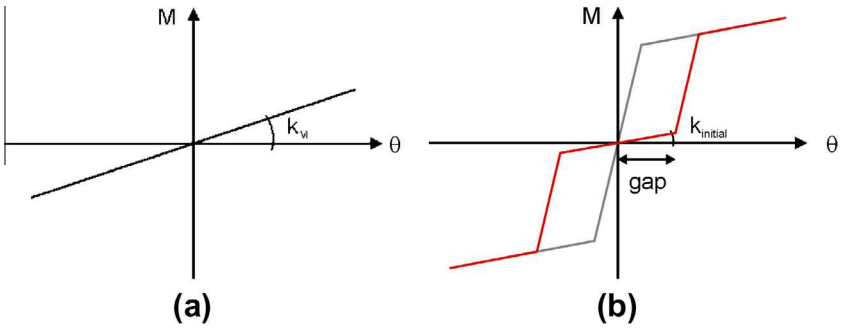

Fig. 15. Joint moment–rotation relationship for: (a) Pinned beam–column joints. (b) Semi-rigid beam–column joints.

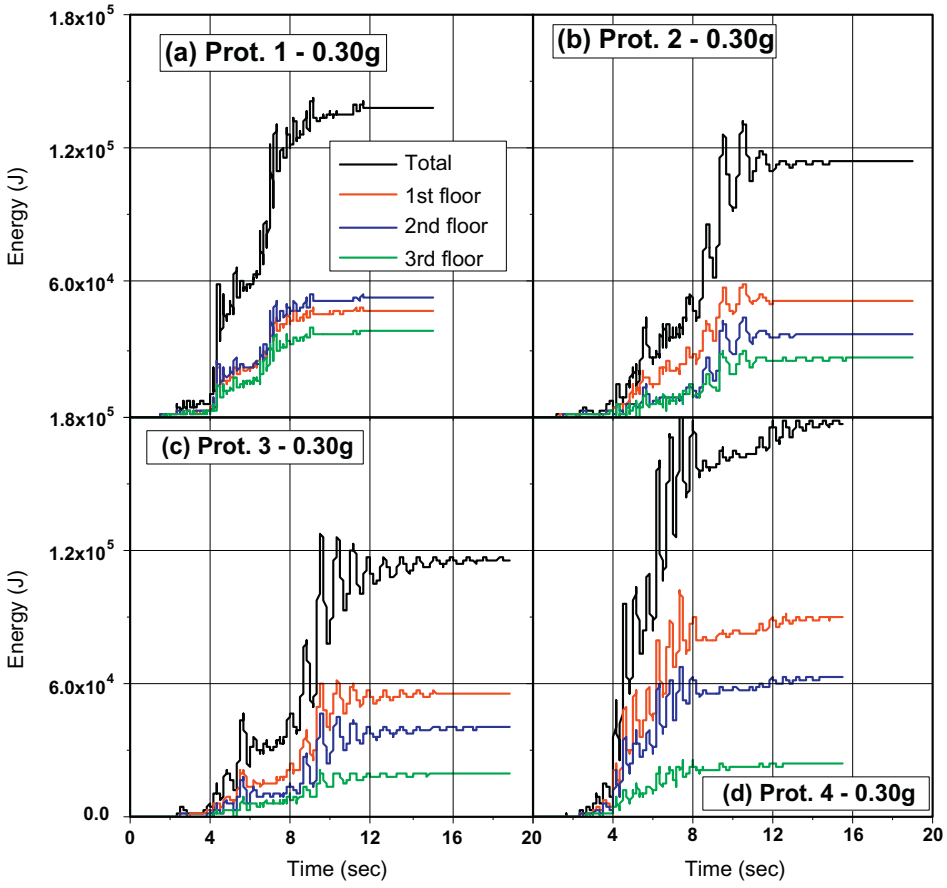

Fig. 16. Total and cumulative energies dissipated in each floor at PGA of 0.30 g, for: (a) Prototype 1. (b) Prototype 2. (c) Prototype 3. (d) Prototype 4.

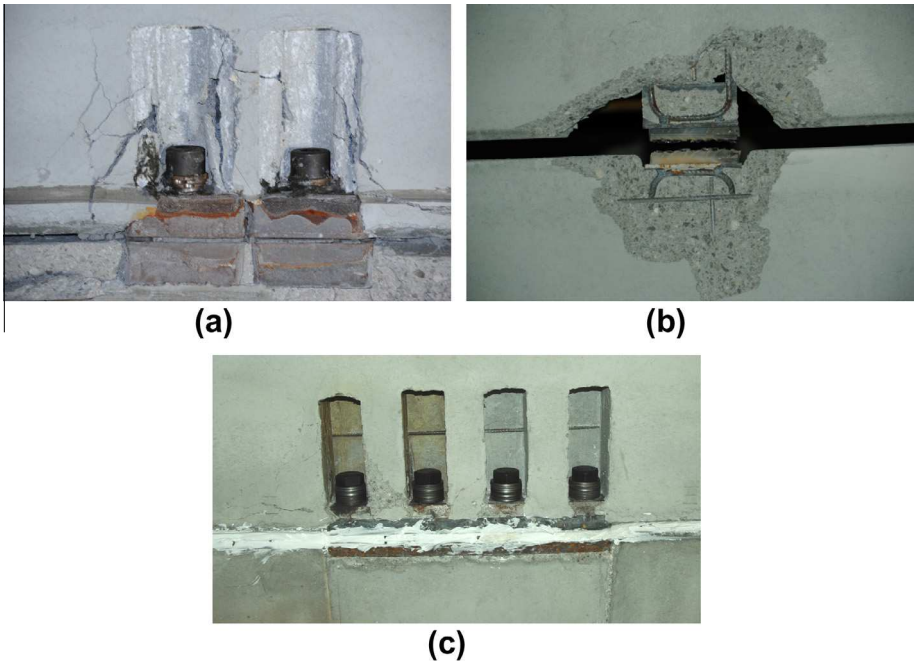

Fig. 17. Damages detected after the cyclic tests: (a) Cracking in the vicinity of the mechanical connector. (b) Broken slab-to-slab welded connections at the first floor.

were identified at the end of the cyclic tests, as shown in Fig. 17a and b illustrates some of the broken slab-to-slab welded connections of the first floor (Fig. 5a), after the cyclic test in prototype 4. Note that this type of failure, that appeared only in the peripheral (4 out of 12) welded slab-to-slab connections of the first floor, did not finally affect at all the effectiveness of its rigid diaphragm.

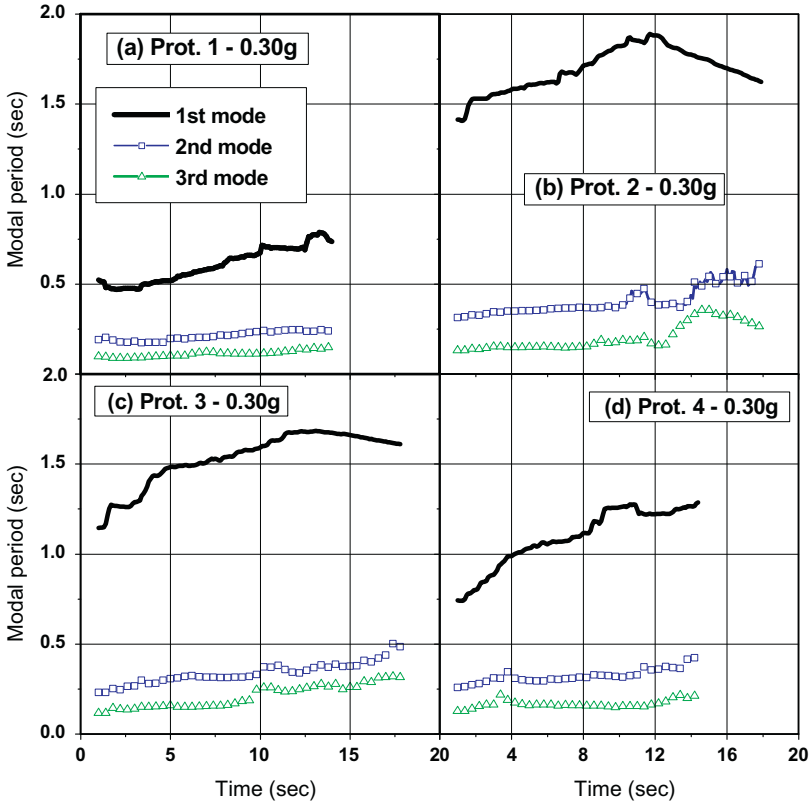

Fig. 18. Evolution of the so-estimated time-varying effective periods of the three modes at PGA of 0.30 g, for: (a) Prototype 1. (b) Prototype 2. (c) Prototype 3. (d) Prototype 4.

5. Modal decomposition of prototype's response

To further investigate the influence of the hinged and emulative beam–column connections on the seismic behavior of the four prototypes, a modal decomposition was executed. The procedure in [16,17] was applied to compute how the effective period of the three modes of the test structures in the direction of testing evolved during the seismic response: a secant stiffness matrix, K, and a viscous damping matrix, C, based on the same DoFs as in the PsD test is fitted by least squares, to the measured restoring force vector, R, and the imposed vectors of displacement and velocity, d and v, respectively, as $R = Kd + Cv$. Note that the PsD equation of motion was formulated without viscous damping, but now this equivalent linear model with viscous damping is used for different purposes.

The identification of the matrices was done repeatedly from the experimental data of a moving time-window on the PsD test results. On the basis of the fitted stiffness matrix, K, and damping matrix, C, and of the theoretical mass matrix M (companion paper), complex eigenvalues and modes were obtained for the central instant of every time-window. Fig. 18 shows the evolution during the tests of the so-estimated time-varying effective periods of the three modes for all prototypes subjected to the 0.30 g earthquake. It is clear from comparing Fig. 18a and b that the initial stiffness of prototype 1 was reduced considerably when the two shear walls were disconnected from the mock-up. The initial value of the prototype's 1st modal period (0.46 s) was increased by a factor of about 3 in its counterpart with hinged beam–column joints (1.41 s). When the beam–column joints of the top floor were restrained, the modal period of prototype 3 was 1.08 s, i.e. 23% shorter than prototype 2, whereas in the case of emulative beam–column-joints (prototype 4), the effective period of the building was 0.66 s (Fig. 18d), approximately half the period measured in prototype 2.

Fig. 19a–d presents the response history of the 3-DoF system to the applied ground motion of 0.30 g in each of the four structural layouts, by applying modal decomposition according to the matrices obtained by the spatial model [17] from time-varying real modes determined from the mass matrix and a symmetric version of the identified stiffness matrix. The modal contributions to the total response for each DoF are plotted in terms of roof displacement and base shear. Regarding the roof displacement response, the contribution of the first vibration mode was prevalent. The first mode contribution is practically equal to roof's total displacement for all prototypes.

On the other hand, regarding the total base shear, Fig. 19a shows that the response of the dual wall-frame precast system involves only the first mode, while Fig. 19b illustrates that in the structural configuration with pinned beam–column joints, the base shear response strongly involves modes 1 and 2. In particular, in prototype 2 the first vibration mode was prevalent for the base shear during the first 3 s of the accelerogram; then the second mode started affecting dominantly the base shear response. It can be observed that up the time step $t = 8.3$ s of the accelerogram, the base shear attributed to the second vibration mode fits very well the total base shear force. Afterwards, the contribution of mode 2 attenuates and mode 1 gives the predominant contribution again. The realization of emulative joints at the top floor in prototype 3, although did not change essentially the global response parameters (maximum base shear; interstorey drifts), disembarrassed the total base shear response from the second and third vibration mode (Fig. 19c). Finally, the activation of the mechanical connectors in every beam–column joint (prototype 4) resulted in a PsD response which was practically attributed exclusively to the

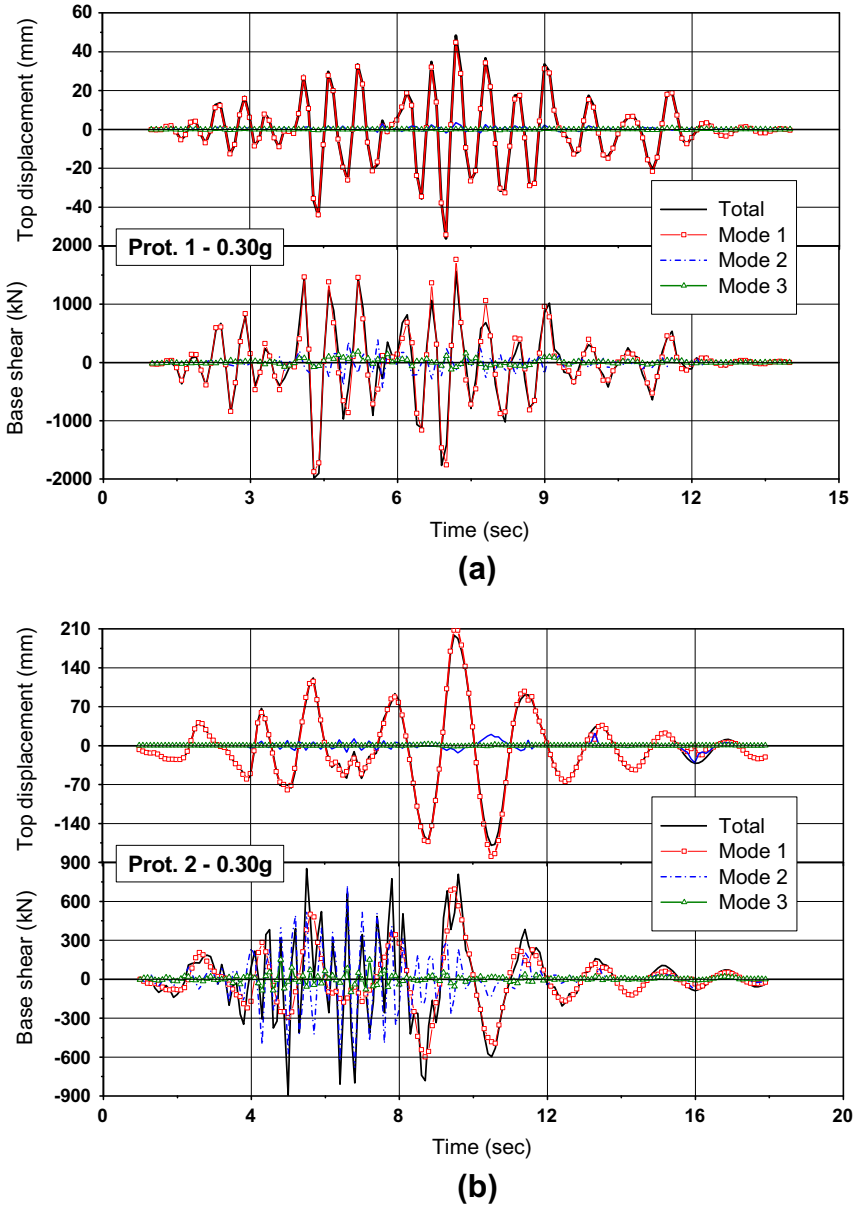

Fig. 19. Modal contribution response history of the 3-DoF system-in terms of roof displacement and base shear-to the applied ground motion of 0.30 g, for: (a) Prototype 1. (b) Prototype 2. (c) Prototype 3. (d) Prototype 4.

first vibration period. As can be seen in Fig. 19d, the component of the 2nd and 3rd mode practically disappeared from the total base shear time histories.

Fig. 20 illustrates the modal contribution response history to the applied ground motions of 0.15 g and 0.30 g for prototype 2 at the second storey force. For each one of the three modes, its contribution is plotted (black line) together with the total response (blue[1] line). This structural configuration with pinned beam–column joints, which was most influenced by the higher modes, has the highest interest for what concerns the storey forces and consequently the design shear forces for the beam–column connections. It is clear from comparing Fig. 20a and b that by doubling the earthquake intensity from 0.15 g to 0.30 g, the second storey forces attributed to the first vibration mode are practically the same, whereas the corresponding forces attributed to mode 2 are more than double for the 0.30 g intensity. This explains the approximately double (total) storey forces for the 0.30 g in comparison with the 0.15 g seismic excitation (Table 2), a fact that should be carefully considered in the design of multi-storey systems, where the simplification of reducing the storey forces by q might not be adequate.

The problem of the large storey forces, and thus of the large actions on connections for the hinged multi-storey structure, had been anticipated by the preliminary numerical simulations and then verified experimentally and should be adequately reflected in design. The magnification factors for the storey forces, which determine the demand on connections, were very high in all stories of prototype 2. If the designer does not include shear walls in these flexible systems (i.e. solution of prototype 1), the large magnification of storey forces (determining the capacity design of connections) should be considered. A possible conservative simplification could be to multiply the design forces in all stories by q.

[1] For interpretation of color in Fig. 20, the reader is referred to the web version of this article.

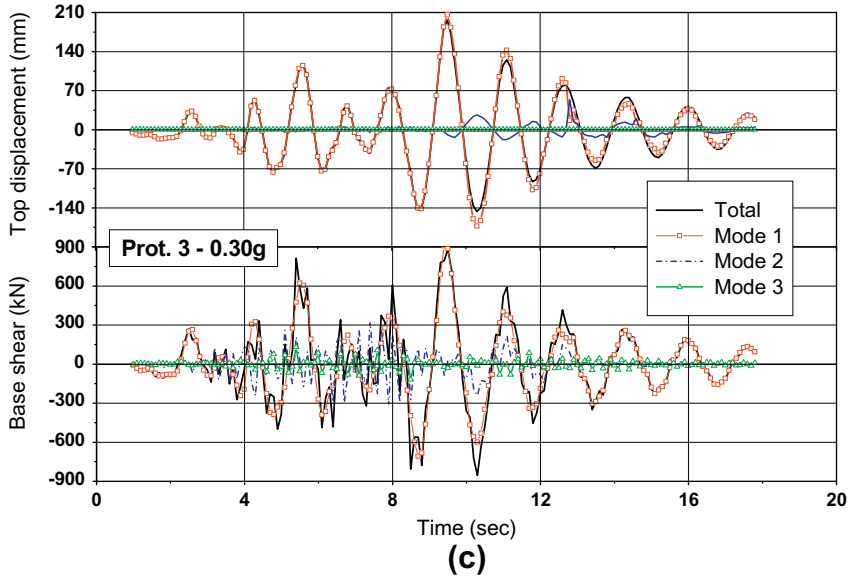

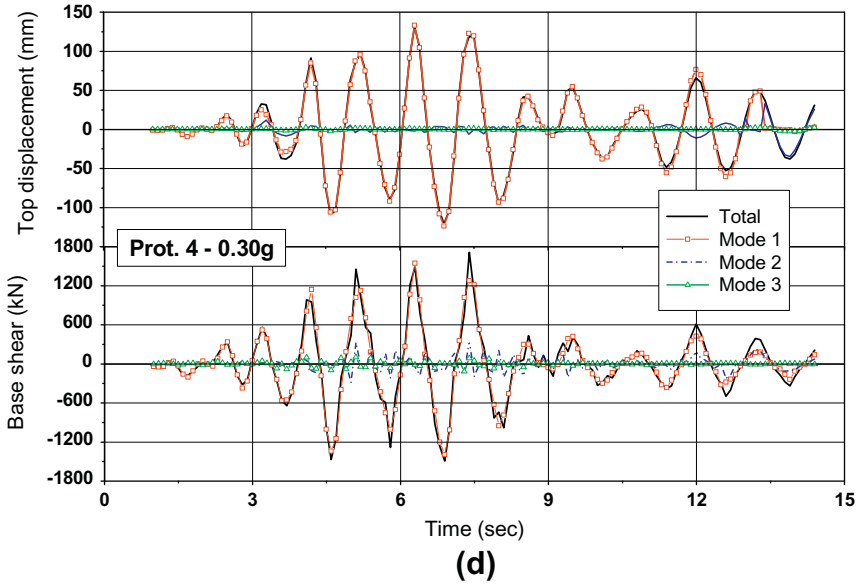

Fig. 19 (*continued*)

6. Conclusions

A full-scale three-storey precast building was subjected to a series of PsD tests in the European Laboratory for Structural Assessment. The mock-up was constructed in such a way that four different structural configurations were investigated experimentally. Therefore, the effect of two types of beam–column connections on the seismic behavior of the three-storey precast building was evaluated. Firstly, the most common connection system in the construction practice in the European countries, comprising pinned beam–column joints, was assessed. Afterwards, the possibility of achieving emulative moment resisting frames by means of a new connection system with dry connections was investigated. The main conclusions are summarized as follows:

- It has been shown that in the case of multi-storey buildings with hinged beam-to-column connections (prototype 2), due to the participation of the higher modes, there is no clear upper limit for the storey forces when the structure enters into the nonlinear regime, as one would expect as a consequence of ductility. This results into large (i.e., much larger than those divided by the q factor) forces in the connections. If the designer does not include shear walls in these flexible systems, the large magnification of storey forces (determining the capacity design of connections) should be considered.
- The rigidity of the first and second's floor (continuous) diaphragms without concrete topping was not impaired by their connection with stiff RC walls. The openings in the diaphragm of the third floor reduced its in-plane stiffness and led to approximately 20% stiffer external frames in respect to the central one. Without shear walls (prototypes 2, 3 and 4), however, the third floor's diaphragm action was substantially improved with equal horizontal displacement in the three frames (Table 3).
- The large in-plane stiffness of the floor (rigid diaphragm), and the elastic response of the connections (stronger connections than elements), allowed for equal distribution of the storey forces among all columns.

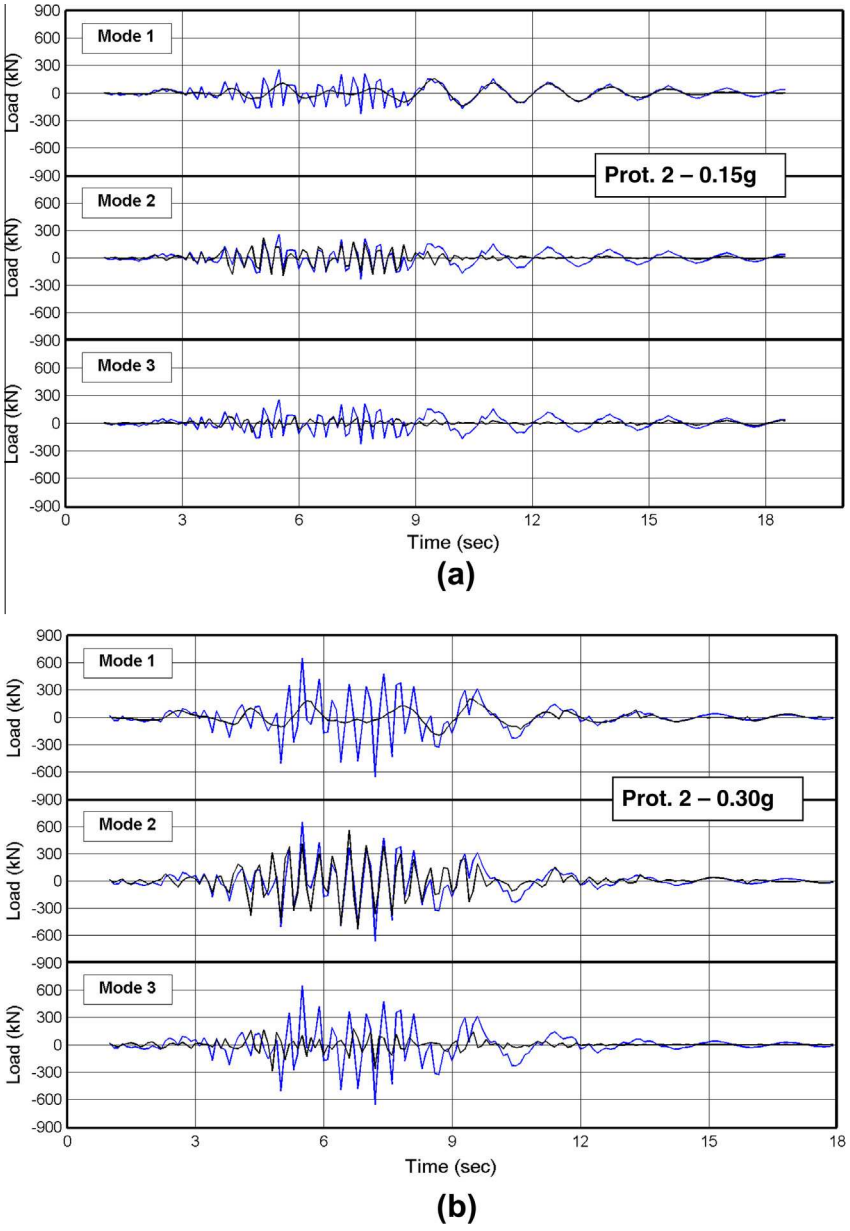

Fig. 20. Modal contribution response history of the second storey force of prototype 2 to the applied ground motions of: (a) 0.15 g. (b) 0.30 g.

- The beam–column joint slip was reduced dramatically in the case of moment resisting joints, that is 3.5 times lower than its counterpart with hinged beam-to-columns joints.
- The participation of the beams in the frame behavior of prototype 4 was higher, however; the emulative beam–column joint response in prototype 4 was quite different from a rigid joint. The execution of this mechanical connection has no quality control or certification for the time being. This resulted into a semi-rigid beam–column joint with asymmetric (in the two directions of loading) and unequal (between beams and columns) rotations.
- Looking at prototype 1 in comparison with its counterpart prototype 2, with hinged beam–column joints but without shear walls, the stiffness was reduced by a factor of about 3. In the case of emulative beam–column-joints (prototype 4), the effective period of the building was half of the period calculated in prototype 2.
- Finally, the contribution of the first vibration mode was prevalent in the roof displacement response – it was practically equal to roof's total displacement for all prototypes. Regarding the total base shear, the response of the precast system with shear walls involves only the first mode, while in the structural configuration with pinned beam–column joints, the response strongly involves modes 1 and 2. Finally, the activation of the mechanical connectors in each beam–column joint resulted in a PsD response which was newly attributed to the first vibration period.
- The analysis of the experimental results, along with the other activities conducted as a part of the SAFECAST project allowed a series of guidelines for the design of connections for seismic actions in precast structures to be drafted [18].

Appendix A

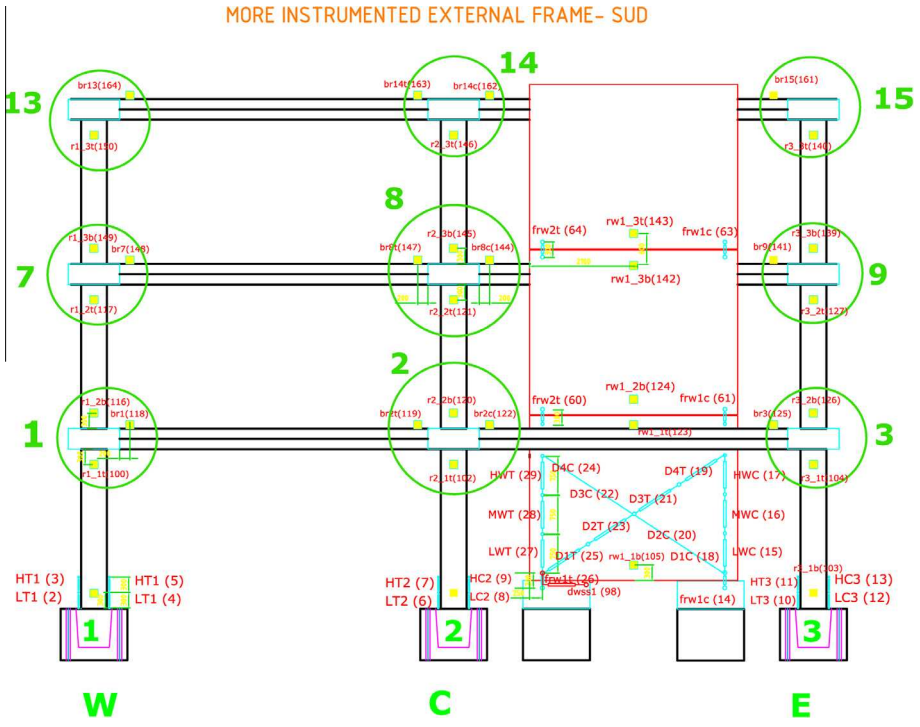
MORE INSTRUMENTED EXTERNAL FRAME- SUD
13
14
15
8
7
9
2
1
3
br13(164)
br14t(163)
br14c(162)
br15(161)
r1_3t(150)
r2_3t(146)
r3_3t(140)
r1_3b(149)
br7(148)
r2_3b(145)
br8t(147)
br8c(144)
br9(141)
r3_3b(139)
r1_2t(137)
r2_2t(121)
r3_2t(127)
r1_2b(116)
br1(118)
r2_2b(120)
br2t(119)
br2c(122)
br3(125)
r3_2b(126)
r1_1t(100)
r2_1t(102)
r3_1t(104)
frw2t (64)
rw1_3t(143)
frw1c (63)
rw1_3b(142)
frw2t (60)
rw1_2b(124)
frw1c (61)
rw1_1t(123)
HWT (29)
D4C (24)
D4T (19)
HWC (17)
D3C (22)
D3T (21)
MWT (28)
MWC (16)
D2T (23)
D2C (20)
LWT (27)
D1T (25)
rw1_1b(105)
D1C (18)
LWC (15)
r2_1b(103)
frw1t (26)
dwss1 (98)
HT1 (3)
LT1 (2)
HT1 (5)
LT1 (4)
HT2 (7)
LT2 (6)
HC2 (9)
LC2 (8)
frw1c (14)
HT3 (11)
LT3 (10)
HC3 (13)
LC3 (12)
1
2
3
W
C
E

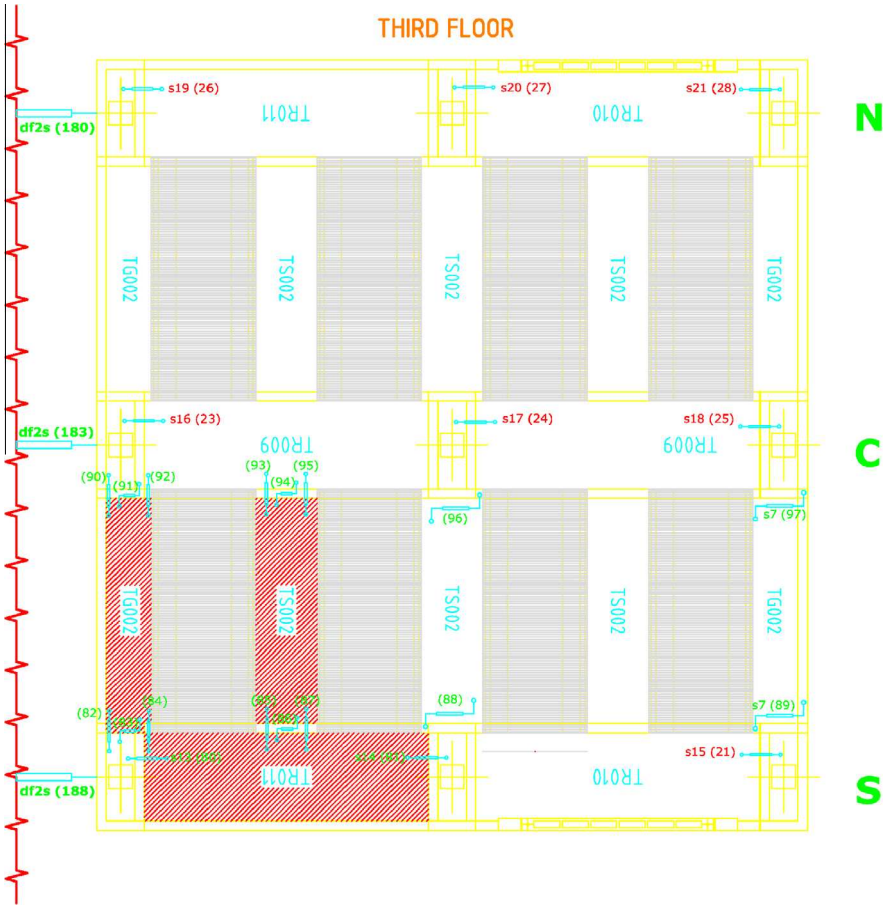
THIRD FLOOR
s19 (26)
s20 (27)
s21 (28)
df2s (180)
TR011
TR010
N
TG002
TS002
TS002
TS002
TG002
df2s (183)
s16 (23)
s17 (24)
s18 (25)
TR009
TR009
C
(90)
(91)
(92)
(93)
(94)
(95)
(96)
s7 (97)
TG002
TS002
TS002
TS002
TG002
(82)
(84)
(88)
s7 (89)
s15 (21)
df2s (188)
TR011
TR010
S

Acknowledgements

The research has been addressed within the SAFECAST project (Grant agreement no. 218417-2), a three-years project (2009–2012) financed by the European Commission within the Seventh Framework Programme. The authors wish to thank the whole ELSA technical team for their assistance in the experimental programme.

References

[1] ATC-08. In: Proceedings of a workshop on design of prefabricated concrete buildings for earthquake loads. ATC, NSF; 1981.
[2] Simeonov S, Park R. Building construction under seismic conditions in the balkan region: design and construction of prefabricated reinforced concrete building systems. UNDP/UNIDO project RER/79/015; 1985. p. 335.
[3] Priestley MJN. The PRESSS program: current status and proposed plans for phase III. PCI J 1996;41(2):22–40.
[4] Nakaki SD, Stanton J, Shritharan S. An overview of the PRESS five-storey precast test building. PCI J 1999;44(2):26–39.
[5] Shiohara H, Watanabe F. The Japan PRESS precast concrete connection design. In: 12th WCEE. Aukland; 2000.
[6] Federation International du Beton – fib. Seismic design of precast concrete buildings structures, bulletin 27. Lausanne; 2003.
[7] Sheppard DA. Connections for seismic resistant precast concrete construction. In: Proceedings of a workshop on design of prefabricated concrete buildings for earthquake loads. ATC-08; 1981.
[8] Restrepo J, Park R, Buchanan A. The seismic behaviour of connections between precast concrete elements. Research report 93-3. Christchurch: Department of Civil Engineering, University of Canterbury; 1993.
[9] Negro P, Bournas DA, Molina FJ. Pseudodynamic tests on a full-scale 3-storey precast concrete building: global response. Elsevier Engineering Structures. 2014;58C.
[10] Olgiati M, Negro P, Colombo A. SAFECAST project: definition and analysis of the three-storey precast buildings. In: Proceedings of the 14th ECEE, 2010.
[11] Fischinger M, Kramar M, Isaković T. The selection of the accelerogram to be used in the experimental program-selection of the record for 3-storey full-scale structure to be tested at ELSA, JRC. SAFECAST – UL Report n°4a; 2010. 66p.
[12] Toniolo G. Experimental behaviour of new/improved connections. Part 1: Contribution of Politecnico di Milano (POLIMI). SAFECAST-Deliverable 2.4. Grant agreement no. 218417-2; 2012. p. 49.
[14] Vintzeleou EN, Tassios TP. Behaviour of dowels under cyclic deformations. ACI Struct J 1987;84(1):18–30.
[15] Fischinger M, Kramar M, Isaković T. Generalization of results to different structures contribution of the University of Ljubljana (UL). SAFECAST-Deliverable 5.2. Grant agreement no. 218417-2; 2012. p. 229.
[16] Molina FJ, Magonette G, Pegon P, Zapico B. Monitoring damping in pseudo-dynamic tests. J Earthq Eng 2011;15(6):877–900.
[17] Molina FJ. Spatial and filter models. MATLAB functions freely available at MATLAB central file exchange. Natick, Massachusetts (USA): The MathWorks, Inc.; 2011. <http://www.mathworks.com/matlabcentral/fileexchange/32634> [August 22].
[18] Negro P, Toniolo G. Design guidelines for connections of precast structures under seismic actions, report EUR 25377 EN, European Commission; 2012. <http://elsa.jrc.ec.europa.eu/publications/LBNA25377ENN.pdf>.